Instrumentation of geogrids using novel non-invasive electrical sensing

Trigg Sharp[1*], *Christos* Mias[1], *Kasia* Zamara[2] and *Gary* Fowmes[1]

[1]School of Engineering, University of Warwick, Library Road, Coventry, CV4 7AL, UK
[2]Tensar International, Sett End Rd W, Blackburn BB1 2PU, UK

Abstract. Accurate strain measurement of geogrids has been challenged by several factors, many of which are due to the unfavourable environmental conditions which geosynthetics are subject to. Existing contributions have seen deployment of standard strain measurement techniques including piezoresistive and fibre-optic sensors. These have faced limitations with poor survivability, low accuracy, and changes to the physical geogrid structure which subsequently alter geogrid behaviour. This report presents a novel, non-invasive, electrical sensor designed for use on geosynthetics specifically. A direct shear apparatus (DSA) was used to apply confining pressure up to 300kPa and strain up to 9.0% to the sensor-enabled geogrids in both dry and wet soil conditions to assess the performance of the novel sensor. Signal phase angle was measured at a range of frequencies at 1mm DSA intervals. Geogrid strain was derived from DSA displacement and a linear response between phase angle and strain has been observed. The findings of this study indicate that the sensor is sensitive to strain and resistant to adverse environmental conditions without modification to the geogrid structure. This is significant as it means that the sensor can be used for instrumentation in field-based applications, particularly where the geogrid is used for soil stabilisation.

1 Introduction

There is an ongoing requirement for the development of instrumentation suitable for use in geosynthetic applications both in research and in industry. Accurate measurement of mechanical parameters, in particular but not limited to strain, can allow for design improvements, real time monitoring, connected infrastructure, disaster recovery, maintenance scheduling, and structural health monitoring of geosynthetic-reinforced structures. Existing, commercially available, sensors have faced issues in use on geosynthetics due to poor strain transferal, susceptibility to damage, and poor adhesion. Instrumentation must achieve 3 main criteria:

- Resilient: Must survive in harsh environments for extended periods of time.
- Unobstructive: Must not change the behaviour of the geosynthetics, the interaction with the soil, or the overall geosystem. Similarly it must not require additional material or protection that also modify behaviour.
- Accurate: Must correctly report behaviour, multiple systems may be deployed for greater confidence.

* Corresponding author: Trigg.Sharp@warwick.ac.uk

The use of transmission lines as strain sensing devices on geosynthetics has been shown to be effective through isolated testing. To further develop this technology for use in commercial applications, it is necessary to validate the efficacy of the sensing system in adverse environmental conditions, including high confining and shearing forces, as well as presence of moisture in the vicinity of the sensor. This is important to understand as the forces which the geosynthetic are subjected to could result in physical damage to the sensing element while presence of water could affect the signal propagation characteristics of the transmission lines. This report focuses on the testing of sensor-enabled geogrids as a proof of concept to give firm assurance to progress with commercial and research development. To do so, instrumented geogrid samples were tested in a direct shear apparatus. Strain was directly applied to the samples under a range of confining pressure and moisture content values to assess the performance of the sensor in response to these variables.

The results from the tests described within this report are highly encouraging. It has been shown that the sensors are capable of surviving tests at confining pressures up to 300kPa and high soil water contents up to fully saturated conditions. In addition to this, the sensors are capable of continued sensing despite significant damage, indicating that the system is resilient to environmental stresses. The results have been further analysed to demonstrate that the use of applied transmission lines are a plausible and sensitive sensor. This indicates that the novel sensor has distinct advantages over existing sensors used for geosynthetic instrumentation and illustrates the requirement for further development of the system.

2 Background

There have been many attempts made at using incorporating readily available sensors onto geosynthetic substrates for sensing in both laboratory and field-based settings. These sensors include piezoresistive strain sensors, either foil-based or conductive polymer composites, extensometers, inclinometers, and surveying techniques. The efficacy of these systems have been reviewed and form the basis of the research presented herein. The primary issues encountered with the use of these sensors are poor adhesion and strain transferal, low survivability in installation, poor resistance to environmental moisture and chemicals, and inherent changes to the geosynthetic functionality.

State-of-the-art geosynthetic strain measurement has focused on fibre-optic based solutions. These sensors typically make use of two principles, either Fibre Bragg Gratings (FBGs) or Brillouin optical time-domain reflectometry or analysis (BOTDR and BOTDA). FBGs allow for discrete, local, measurement of strain while distributed fibre-optic strain sensing, based on Brillouin scattering, allows for spatially continuous strain measurements along the length of optical fibres which are bonded to structures [1]. Importantly, the use of fibre optics poses low environmental hazards as they are chemically inert as well as corrosion resistant. While fibre optic sensors are immune to electromagnetic interference, they are affected by temperature and therefore require a strain-independent sensor to remove measurement errors caused by temperature fluctuations. The specific principles which allow for fibre optics to act as strain sensing elements are beyond the scope of this report, but the general mechanism is that there is a variation in the frequency of the transmitted or internally reflected light spectra of a fibre optic when it is subjected to mechanical strain. The shift in frequency is then measured and calibrated against strain to allow for strain to be measured in the cable.

For use in geogrids, the fibre optic elements can either be applied to, using adhesives [2], or woven within [3] geogrid ribs. If applied externally, care must be taken to add protection to the fibre optic as the elements are fragile and sensitive to mechanical damage. If there is damage to any section of the cable, the signal will be unable to propagate further, limiting the effectiveness of sensing. This is also the case for fibre optic elements which are woven into the geogrid ribs and recent tests have had to use a geotextile element to protect the ribs from damage to ensure integrity of the embedded fibre optics [4]. The need to protect the embedded cables with geotextiles critically alters the function of the geogrid as it closes the apertures of the grid to large soil particles, reducing the interlocking and confinement effects associated with the stabilisation property of geogrids.

The development of a novel strain sensor which is designed for use on geosynthetics poses as a unique alternative to the existing focus on fibre optic systems. Further works are required to further understand the performance of the sensor in different environments and configurations. The requirement to investigate transmission line strain sensors in the conditions presented in this report is due to the unique structure and sensing principle of the sensor. The underlying sensing principles associated with these sensors will only be covered in brief to provide context for the study presented herein. Phase-based transmission line strain measurements are defined by Equation 1 which allows strain to be calculated indirectly from change in sensor length Δl by measuring change in phase angle $\Delta\phi$. Strain-phase sensitivity $\Delta l/\Delta\phi$ is proportional to phase constant β which iself is a function of signal frequency ω as shown in Equation 3.

$$\Delta\phi = -\beta\Delta l \tag{1}$$

In utilising Equation 1, it is assumed that the propagated signal is entirely confined within the sensor trace and geosynthetic dielectric and does not interact with the surrounding medium. This can be encouraged by applying a thick insulating coating to the sensor trace to physically isolate and distance the trace from any lossy media surrounding the sensor. Further to this, the conductive coating should be designed to meet a minimum thickness of 5 skin depths δ, calculated for the maximum sensing frequency using Equation 2, to further mitigate electric (E) and magnetic (H) field interaction with the surrounding lossy media. Material parameters μ_c and σ_c are the permeability and conductivity of the conductor respectively.

$$\delta = \frac{1}{\sqrt{(\pi f \mu_c \sigma_c)}} \tag{2}$$

Equation 3 shows that β is dependent on the transmission line parameters L', G', R', and C' which correspond to the inductance, conductance, resistance and capacitance per unit length of the line respectively. The per unit parameters are affected by the permeability μ, permittivity ε and conductivity σ of the transmission line media.

$$\beta = \mathrm{I}\left[\sqrt{\left((R' + j\omega L')(G' + j\omega C')\right)}\right] \tag{3}$$

where I[...] stands for imaginary part of of the complex attenuation constant of the transmission line γ.

Changes to the surrounding media caused by water ingress or other soil changes will result in a change in β and subsequent $\Delta\varphi$. Further to this, confining pressure on the sensor may cause changes in capacitance C' as the dielectric thickness may vary as pressure is applied.

The effects described establish a clear requirement for study. While steps have been taken to mitigate the effects of lossy environmental media, it is necessary to evaluate whether the sensor is still suitable for utilising in these conditions. It is anticipated that, for variable soil conditions, a strain-independent transmission line probe will have to be adopted and used to calibrate out any environmental effects as is performed for temperature in fibre optic sensors.

3 Methodology

A simple test regime used to evaluate transmission line sensors in harsh environmental conditions. Test samples were produced as proof-of-concept models using RE540 geogrid elements provided by *Tensar International*.

3.1 Sample Manufacture

Geogrid samples were first plasma treated under vacuum using a *Henniker Plasma Nebula* unit at 0.1mbar in order to clean the surfaces from contaminants such as oils and dust. The additional role of the plasma treatment is to increase the surface free energy of the substrate material in order to improve adhesion of coatings. It is recommended that plasma treatment, either atmospheric or vacuum, is used to prepare geosynthetics produced from inert polymers such as PP or PET before applying any adhesive or coating, regardless of application.

A jig was used to apply light tension to a sample of geogrid to ensure that any coatings were applied perpendicular to the surface. A polyolefin adhesion promoter (PAP) was sprayed onto the sample to aid strong adhesion of any coatings. Conductive flex paint, containing silver flake particles, was then applied to either side of a single geogrid rib along the required test length to form the parallel plate transmission line. For the samples tested in this report, the paint was brushed onto the substrate manually. The paint was allowed to cure in the jig under tension.

50Ω Sub-Miniature A (SMA) connectors were then bonded to the ends of the transmission line using cyanoacrylate and, once cured, were cold soldered to the conductive paint traces to allow connection to electronic equipment. Edges of the ribs were trimmed using a sharp scalpel blade to remove any paint overspill which would cause shorting of the sensor's two conductors. SMA connectors were then masked and the entire geogrid was treated with a conformal coating. Five coating layers were applied to ensure sufficient thickness.

3.2 Direct Shear Apparatus Testing

A 300 mm direct shear apparatus (DSA), was used to directly strain the samples within a soil confinement. Before placing the sample into the DSA, measurements of the trace resistance for each trace were taken using a multimeter to ensure good conductivity. The geogrid samples were mounted to the DSA using mechanical tensioners and were embedded within a sharp sand soil that was compacted as it was added to the DSA setup to remove any large voids

Following soil placement, the geogrid was connected to a PicoVNA 106 Vector Network Analyser (VNA) with 50Ω coaxial SMA cables. The VNA was calibrated using a Short-Open-Line-Through (SOLT) calibration method. Subsequently, the VNA was used to send a range of frequencies through the geogrid sensor from 100MHz up to 6GHz. Over this frequency range, the VNA measures the phase shift and attenuation of the signal as it travels therought the sensor. The DSA was set to the required strain rate and confining pressure for the tests as shown in Table 1. For tests 3 and 4, the soil was wetted and mixed before being placed in the DSA in several layers. Moisture content was kept at a constant value for the duration of each test and was measured following BS EN 17892-1 both before and immediately after test completion to ensure constant moisture content. Degree of saturation S_r was determined for the soil samples. The DSA was operated at a strain rate of 1.5mm/s up to a maximum displacement of 25mm, with the phase of the system and shear force being recorded at each 1mm increment. Displacement was measured using the LVDT incorporated in the DSA and geogrid strain was derived from this using the measured length of the geogrid sample. VNA output was recorded at each 1mm increment and markers were used across the frequency sweep to measure change in phase angle at specific frequencies.

Table 1. DSA testing conditions.

Test	σ_1 (kPa)	Θ_m (%wt)	S_r (%)
1	200	1.95	10.3
2	300	2.01	10.6
3	100	9.38	49.7
4	200	7.54	40.0

3.3 Large Scale Testing

A simple large scale test was performed with support of the *University of Birmingham* and the *National Buried Infrastructure Facility (NBIF)*. The purpose of the test was to assess the performance of the sensor over a longer measurement length and to test its survivability in an unfavourable aggregate. This test involved preparing a sample of 5m length using the same procedure described in 3.1. The sample was placed onto a soft sand base and was connected to the VNA using 50Ω coaxial cables. Calibration was performed as is described in 3.2 and measurements were taken before progressing. Following this, a recycled aggregate, closely aligned to an oversized 6F5 specification from the Standards for Highway Works Series 600, was placed on top of the sample and compacted using a plate compactor. Measurements were taken after compaction to assess changes to the signal and sensor. Figure 1 shows the sample design and test aggregate.

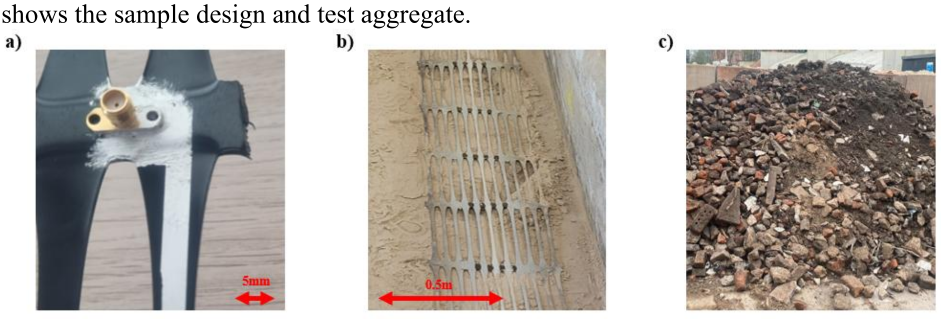

Fig 1. a) A section of geogrid sample showing SMA connector. b) Large scale geogrid sample before aggregate placement. c) Oversized 6F5 specification aggregate.

4 Results

As stated in 3.2, signal phase angle was measured at a range of frequencies to facilitate quantitative analysis during testing. When using a VNA for measurements, the phase represents the delay in signal propagation from input to output of the system. As such, a strained sensor will result in a greater delay between signal input and output across the transmission line. This is reflected in the phase measurement as the phase of the signal will decrease due to the increased signal lag as demonstrated in Figure 2. The ideal response of phase angle to strain is defined by Equation 1, indicating a negative linear relationship between the variables. As β is a function of frequency ω, the magnitude of slope gradient for the phase angle change should increase as the signal's frequency increases.

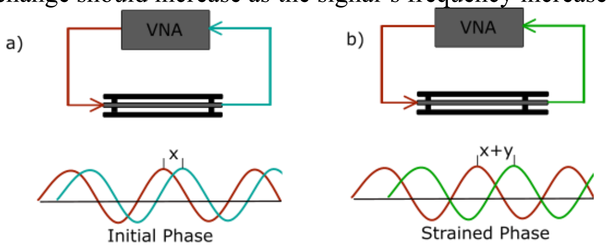

Fig 2. Demonstration of phase shift. a) In unstrained state, there is delay between incident (red) and received (blue) signal represented by phase angle -*x*. b) Strain increases delay between incident (red) and received (green) signal, resulting in phase of –(*x*+*y*).

It should be noted that, as the measurements are uncalibrated against mechanical strain, the R^2 values are only representative of the phase trends in response to strain and are only valid for low strain values. For embedded phase angle measurements, the phase-strain response will be non-linear due to reflections and scattering however de-embedded measurements generated using improved calibration methods will be perfectly linear. Use of R^2 values is based off the approximation that embedded results will still follow a generally linear trend despite transmission line effects causing interference. The simulated difference between the embedded and de-embedded response is shown in Figure 3.

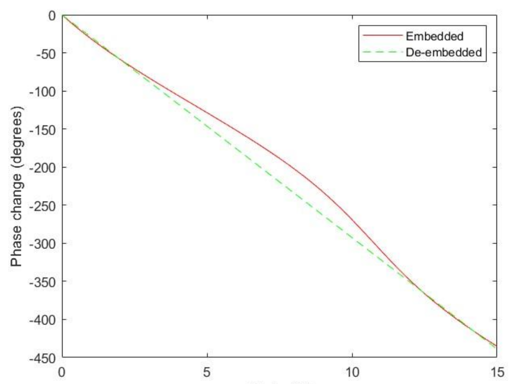

Fig 3. Plot showing the simulated difference in phase angle response to mechanical strain between embedded and de-embedded transmission lines.

4.1 DSA Results

4.1.1 Test One

The measured resistances of the traces were 11.3Ω and 17.4Ω. The total displacement of the DSA was 27.04mm which resulted in 9.01% final strain in the sample. The R^2 value for the 1500MHz, 4500MHz, 6000MHz, and Average markers are 0.973, 0.976, 0.993, and 0.988 respectively, indicating a highly linear relationship between strain and phase angle. The slope coefficients of the trendlines were -10.5, -26.0, -35.6, and -23.6 respectively, indicating that the rate of change of phase angle in response to strain is dependent on the measurement point frequency, which is expected, based on equation 3, as the phase constant is a function of the frequency. The response plot is provided in Figure 4.

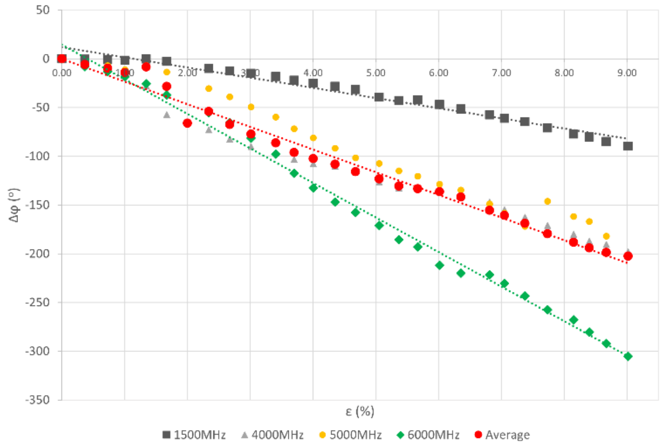

Fig 4. Test One plot of Δφ against ε showing clear linear response in phase angle in response to strain application. The effect of higher frequency measurement points on the sensitivity of the sensor is evident.

4.1.2 Test Two

The measured resistances of the traces were 9.5Ω and 8.6Ω. The total displacement of the DSA was 20.43mm which resulted in 6.81% final strain in the sample. The R^2 value for the 1500MHz, 5000MHz, and Average markers are 0.491, 0.954, and 0.930 respectively, indicating a highly linear relationship between strain and phase angle for most markers. The slope coefficients of the trendlines were -1.85, -15.1, and -13.3 respectively, further indicating that the rate of change of phase angle in response to strain is dependent on the measurement point frequency. The response plot is provided in Figure 5.

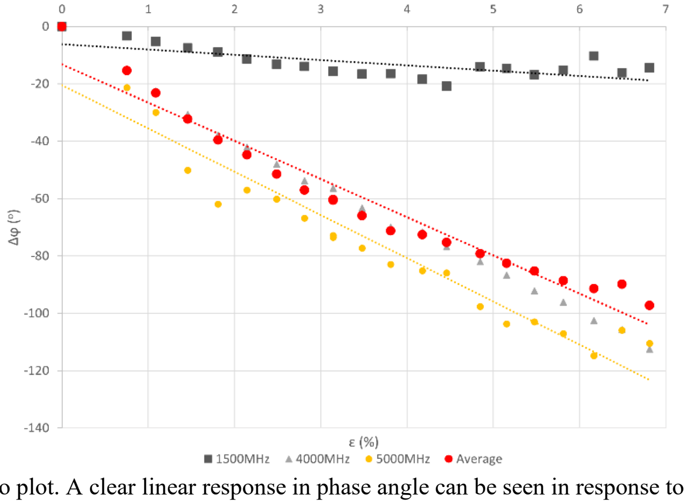

Fig 5. Test Two plot. A clear linear response in phase angle can be seen in response to strain across all frequency points, with higher frequency points more sensitive to strain.

4.1.3 Test Three

The measured resistances of the traces were 6.7Ω and 7.1Ω. The total displacement of the DSA was 12.99mm which resulted in 4.33% final strain in the sample. The R^2 value for the 3005MHz, 3094MHz, and Average markers are both 0.994, 0.986, and 0.991 respectively, indicating a highly linear relationship between strain and phase angle in wet soil conditions. The slope coefficients of the trendlines were -24.8, -25.3, and -25.0 respectively. The response plot is provided in Figure 6.

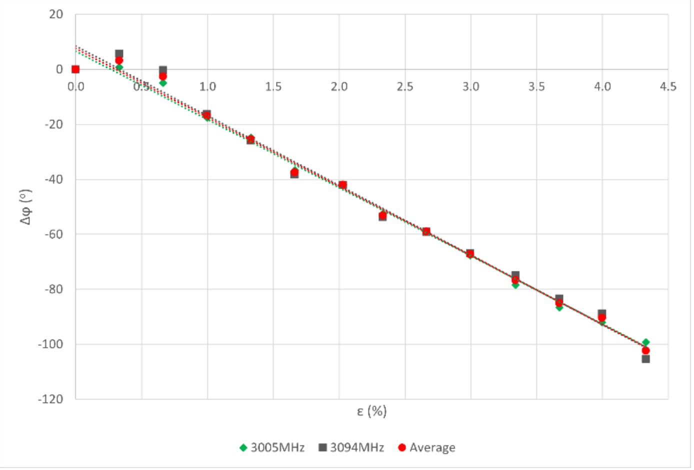

Fig 6. Test Three plot showing a highly linear response for both marker points, indicating that strain measurement is suitable even in moist soil conditions.

4.1.4 Test Four

The measured resistances of the traces were 193Ω and 296Ω. The total displacement of the DSA was 25.03mm which resulted in 8.34% final strain in the sample. The 1500MHz marker shows no perceptible change in response to strain while the 4500MHz marker point is significantly affected by random noise. The 3000MHz and 3250MHz marker points show a similar linear response after 2.0% recorded strain. The response plot is provided in Figure 7.

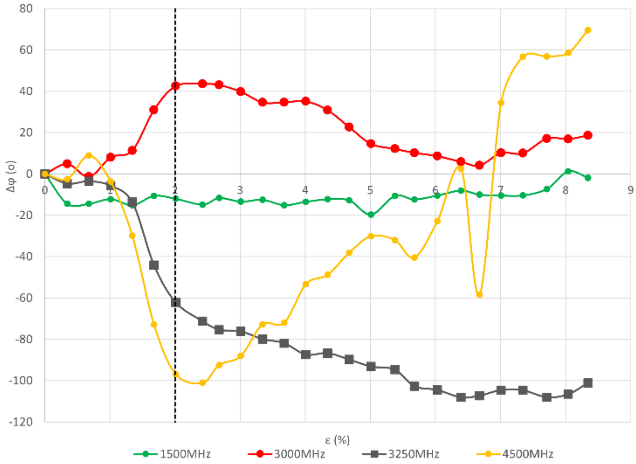

Fig. 7. Test Four plot. Significant noise can be observed across all frequencies. A gentle linear response can be observed in the midrange after 2.0% strain, indicating that the geogrid may not have been taut in installation.

4.2 Large Scale Results

Two sensor lines were interrogated, each of 5m length. Sensor 1 had trace resistances of 15.5Ω and 18.1Ω. Sensor 2 had trace resistances of 24.1Ω and 23.5Ω. Prior to aggregate placement, peak S21 signal strength was -28dB and -40dB for Sensors 1 and 2 respectively. Phase plots were recorded for each trace and closely match theoretical predictions. Placement and compaction of the aggregate caused severe damage to the connectors and connection detail of the transmission lines as shown in Figure 8, nullifying any subsequent measurements. Sensor traces were manually investigated for damage and no significant issues were observed.

Fig 8. Large scale test sample following excavation. Arrows show location of connector damage.

5 Discussion

Through testing, it has been demonstrated that conductive coatings can be applied to create transmission line traces with very low DC resistance values relative to the 50Ω impedance of the coaxial lines. This indicates that this method of application is suitable for the production of transmission line elements. It is worth noting that the coating thickness must be approximately 5 skin depths, or greater, for a representative EM signal in order to reduce the electromagnetic signal interaction with the surrounding medium. This is particularly important for cases where the sensor will be applied in environments containing soil or moisture, in which case losses will be higher. This highlights the requirement for rigorous quality control in manufacture by accurately measuring the conductive coating thickness and ensuring sufficiently thick and hard external, electrically insulating, coatings.

The results obtained from Tests 1 and 2 both demonstrate that the sensor outputs a linear change in signal phase angle in response to mechanical strain despite confining pressures of 200kPa and 300kPa respectively. This change is consistent with previous tests and simulation results, with comparable markers exhibiting a similar regression coefficient which suggests that the phase response of the system is independent from the confining pressure which it is subjected to. It is worth noting that the rate of change for markers varies between Tests 1 and 2. It is believed that this has arisen from differences in impedance between the samples due to variances in material composition and line geometry through manufacture. This further highlights the requirement for improved standardisation in manufacturing methods and material selection in order to more effectively characterise and improve the sensor elements.

The results obtained from Test 3 shows that the system is capable of identifying mechanical strain applied to the sensor in environments with high moisture contents. This is encouraging in showing that the sensor is capable of functioning in typical civil engineering soil conditions and demonstrates its suitability for industrial sensing applications. There are clear discrepancies in Test 4 which are likely to have arisen as a result of the high DC resistance of the electrical traces. The likely source of this is from the change in conductive coating and singular coating layer. The sample was treated with the acrylic conductive coating which has a resistivity 8x higher than the alternative epoxy-based coating as used in Tests 1-3 which will have resulted in a higher resistance [4, 5]. This identifies the requirement for ensuring that the layer resistance of the sensor traces are sufficiently low for effective sensing. Further electromagnetic simulations are required to validate the findings presented herein. Further to this, it is necessary to investigate any changes to phase angle in response to varied moisture content as Tests 3 and 4 were completed at fixed moisture contents whereas industrial applications will likely experience variable conditions.

It is assumed that the phase angle recorded by the VNA was significantly affected by internal reflections caused by impedance mismatching. This means that, while observation of electrical changes in response to strain is possible, one cannot discern the true strain value using Equation 1 as it is not possible to discern whether the measured phase angle is the true S_{21} measurement, a reflected wave, or a superposition of several incident and reflected waves. Once the geogrid transmission line parameters are better understood, these will be revised to be correctly calibrated. The standard method for removal of errors associated with impedance mismatches is to treat the transmission line element as a device under test (DUT) and de-embed it from the connectors using a suitable calibration method. Through-Reflect-Line (TRL) method can be used for this purpose. The process of de-embedding allows for the effects associated with mismatching of the line to be calibrated out from the system which allows for accurate phase measurement as any erroneous reflections or scattering are removed. This requires further research as all results obtained to date have used SOLT calibration which does not de-embed the DUT.

The large scale test proved successful in showing that low resistance traces could be produced over a large sample length and that attenuation was moderate. Further to this, it was reassuring that minimal damage was sustained by the sample in response to compaction with an unfavourable aggregate. The resistance of the traces remained the same following the test. It further highlighted the requirement to improve the trace-connector interface to prevent detachment of the connectors from the conductive traces.

References

[1] C. Kechavarzi, X. Xu and P. Keenan, Fibre optic sensing systemsforsafer real-time, Cambridge Centre for Smart Infrastructure and Construction, Cambridge, 2023.

[2] K. Zamara, G. Fowmes and J. Kawalec, Geogrid stabilisation application–review of strain measurement methods, research and implications on design approaches, IOP Conference Series: Materials Science and Engineering, **1260**, no. 1, 2022.

[3] X. Xiaomin, K. Cedric, W. David, H. Graham, H. Harmut, D. B. Nicholas, W. Dave, B. Edgar, T. Sarah and S. Nick, Fibre optic instrumented geogrid for ground movement, in Field Monitoring in Geomechanics: 11th International Symposium, London, 2022.

[4] MG Chemicals, 843AR Liquid, MG Chemicals, Burlington, 2024.

[5] Chemtronics, CircuitWorks Conductive Pens & Paint, Chemtronics.

This work was supported by the Engineering and Physical Sciences Research Council [EPSRC EP/W524645/1]